

This article is published as part of the *Dalton Transactions* themed issue entitled:

Dalton Transactions 40th Anniversary

Guest Editor Professor Chris Orvig, Editorial Board Chair
University of British Columbia, Canada

Published in issue 40, 2011 of *Dalton Transactions*

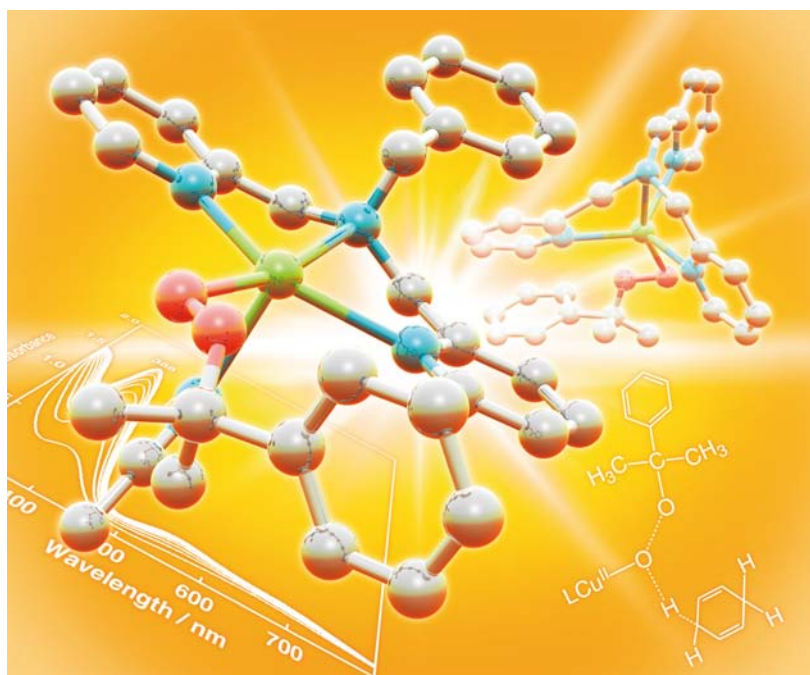


Image reproduced with permission of Shinobu Itoh

Welcome to issue 40 of the 40th volume of *Dalton Transactions*-40/40! Articles in the issue include:

PERSPECTIVE:

[Synthesis and coordination chemistry of macrocyclic ligands featuring NHC donor groups](#)

Peter G. Edwards and F. Ekkehardt Hahn
Dalton Trans., 2011, 10.1039/C1DT10864F

FRONTIER:

[The future of metal–organic frameworks](#)

Neil R. Champness
Dalton Trans., 2011, DOI: 10.1039/C1DT11184A

ARTICLES:

[Redox reactivity of photogenerated osmium\(II\) complexes](#)

Jillian L. Dempsey, Jay R. Winkler and Harry B. Gray
Dalton Trans., 2011, DOI: 10.1039/C1DT11138H

[Molecular squares, cubes and chains from self-assembly of bis-bidentate bridging ligands with transition metal dications](#)

Andrew Stephenson and Michael D. Ward
Dalton Trans., 2011, DOI: 10.1039/C1DT10263J

Visit the *Dalton Transactions* website for more cutting-edge inorganic and organometallic research

www.rsc.org/dalton

Cite this: *Dalton Trans.*, 2011, **40**, 10568

www.rsc.org/dalton

PAPER

Steric control on the redox chemistry of $(\eta^5\text{-C}_9\text{H}_7)_2\text{Yb}^{\text{II}}(\text{THF})_2$ by 6-aryl substituted iminopyridines†Alexander A. Trifonov,^{*a} Boris G. Shestakov,^a Ivan D. Gudilenkov,^a Georgy K. Fukin,^a Giuliano Giambastiani,^{*b} Claudio Bianchini,^b Andrea Rossin,^b Lapo Luconi,^b Jonathan Filippi^b and Lorenzo Sorace^c

Received 24th January 2011, Accepted 5th April 2011

DOI: 10.1039/c1dt10135h

A steric control on the reductive capacity of ytterbocenes towards iminopyridine ligands is described. The reaction of $(\eta^5\text{-C}_9\text{H}_7)_2\text{Yb}(\text{THF})_2$ with a series of 6-organyl-2-(aldimino)pyridyl ligands (IPy) takes place with the replacement of two THF molecules by one IPy unit. In contrast to the rich reductive ytterbocene chemistry described in the presence of the unsubstituted (aldimino)pyridyl ligand, all 6-aryl substituted IPys scrutinized hereafter are involved into the metal coordination as neutral bidentate {N,N} or tridentate {N,N,S; N,N,O} ligands, with no changes of the metal oxidation state in the final complexes. A series of Yb^{II} metallocene complexes of general formula $(\eta^5\text{-C}_9\text{H}_7)_2\text{Yb}^{\text{II}}(\eta^2$ or $\eta^3)[2,6\text{-}i\text{-Pr}_2(\text{C}_6\text{H}_3)\text{N}=\text{CH}(\text{C}_5\text{H}_5\text{N})\text{-6-R}]$ have been isolated and completely characterized. The stereo-electronic role of the aryl substituents in the IPy ligands on the ytterbocene redox chemistry has also been addressed.

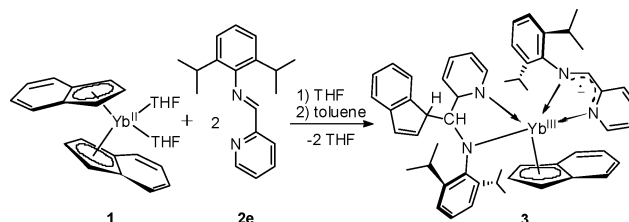
Introduction

Redox-active α,α' -diimines appeared in the literature in the late 1960s as a versatile ligand family capable of providing transition-metal complexes with unusual structures and unique reactivity.¹ Since the 1980s, Cloke and Edelman reported the use of diazabutadiene ligands (DAB) for the preparation of organolanthanide complexes, a study that represented an important milestone in the development of this organometallic area.²

The combination of the redox properties of the DAB ligands³ and ytterbium (for which two stable oxidation states featured by a rather low $\text{Yb}^{\text{II}} \rightleftharpoons \text{Yb}^{\text{III}}$ interconversion potential are possible)⁴ has opened the way to the development of a rich organometallic chemistry. The reactions between ytterbocenes with variable steric hindrance and DAB ligands can follow different reaction paths, resulting into either $\text{Yb}^{\text{II}}/\text{Yb}^{\text{III}}$ oxidation,⁵ formation of unexpected C–C bonds⁶ or C–H bond activation on the ligand skeleton.⁶ The variation of steric hindrance of ytterbocenes is also

known to modulate their reductive properties (from one- to two-electron donor systems) towards DAB ligands.⁷ Finally, the latest progresses in the organometallic chemistry of ytterbium complexes with DAB ligands have contributed to highlight relevant aspects of the complex ytterbium redox chemistry, from the occurrence of solvent-mediated redox transformations^{5b-d} to temperature-induced redox isomerizations.⁷

More recently, some of us have reported on the reactivity of the bis(indenyl) ytterbium complex $(\eta^5\text{-C}_9\text{H}_7)_2\text{Yb}^{\text{II}}(\text{THF})_2$ (**1**) with a DAB-structurally related α -iminopyridine (IPy) ligand (**2e**, Chart 1).⁸ The reaction outlined in Scheme 1 can be formally interpreted as the unprecedented C=N bond insertion into the η^5 -indenyl-Yb bond and metal oxidation to give the $\text{Yb}^{\text{III}}(\eta^5\text{-C}_9\text{H}_7)\{\eta^2\text{-}2,6\text{-}i\text{-Pr}_2(\text{C}_6\text{H}_3)\text{N}=\text{CH}(\text{C}_9\text{H}_7)(\text{C}_5\text{H}_5\text{N})\}\{\eta^4\text{-}2,6\text{-}i\text{-Pr}_2\text{C}_6\text{H}_3\text{N}=\text{CH}(\text{C}_5\text{H}_5\text{N})\}$ species **3** (Scheme 1).^{8a}



Scheme 1 Synthesis of complex 3.

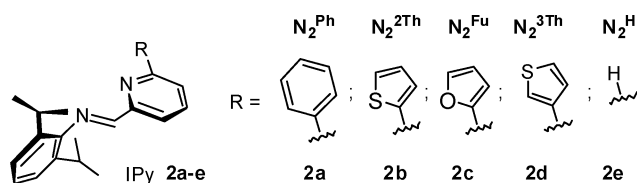
The haptotropic rearrangement of the π -coordinated indenyl fragments seems to be the key-factor driving the observed reactivity. Notably, no imine C=N bond alkylation by the “Cp” anionic ligand is observed when the reaction of **2e** takes place with differently hindered ytterbocene complexes $[\text{Yb}^{\text{II}}\text{bis}(\text{fluorenyl})(\text{THF})_2]$

^aG.A. Razuvaev Institute of Organometallic Chemistry of Russian Academy of Sciences, Tropinina 49, GSP-445, 603950, Nizhny Novgorod, Russia. E-mail: trif@iomc.ras.ru; Fax: (+7) 8314621497

^bIstituto di Chimica dei Composti Organometallici (ICCOM - CNR), Via Madonna del Piano 10, 50019, Sesto Fiorentino, Italy. E-mail: giuliano.giambastiani@iccom.cnr.it; Fax: (+39) 055 5225203

^cDipartimento di Chimica “U. Schiff” and UdR INSTM, Università di Firenze, Via della Lastruccia, 3–13, 50019 Sesto Fiorentino, Italy

† Electronic supplementary information (ESI) available: Complete crystallographic data and tables for complexes **4–7** and UV-VIS spectra of ligands **2a–d** and related Yb^{II} -complexes **4–7**. CCDC reference numbers 794890 (**4**), 795224 (**5**), 794891 (**6**) and 794889 (**7**). For ESI and crystallographic data in CIF or other electronic format see DOI: 10.1039/c1dt10135h



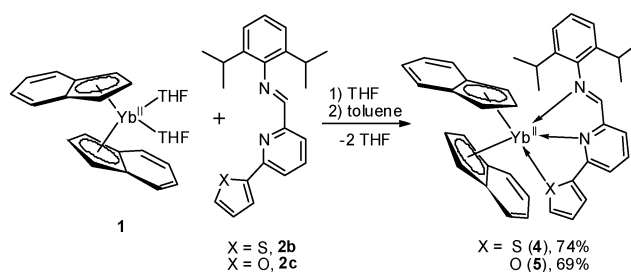
(fluorenyl = $\eta^5\text{-C}_{13}\text{H}_9$)^{6a} or $\text{Cp}_2\text{Yb}^{\text{II}}(\text{THF})_n$ ($\text{Cp} = \text{C}_5\text{Me}_5$, $\text{C}_5\text{Me}_4\text{H}$, C_5MeH_4)^{8b}]; in these cases, variably substituted Yb^{III} products have been isolated and completely characterized. Overall, the reactions of ytterbocenes with **2e** have proven to be strongly dependent on the bonding nature of $\text{Yb}\text{-}\eta^5$ -coordinated aromatic groups. In contrast to this general assessment, the role of the IPy ligand and its stereo-electronic properties in the reaction with ytterbocenes still remains unknown. In order to get more insights on this specific point, we report hereafter on the reactivity of the $(\eta^5\text{-C}_9\text{H}_7)_2\text{Yb}(\text{THF})_2$ complex (**1**) with a series of 6-organyl-2-(aldimino)pyridyl ligand derivatives (**2a–d**, Chart 1). A number of divalent ytterbium complexes of general formula $(\eta^5\text{-C}_9\text{H}_7)_2\text{Yb}^{\text{II}}(\eta^2 \text{ or } \eta^3)[2,6\text{-Pr}_2(\text{C}_6\text{H}_3)\text{N}=\text{CH}(\text{C}_3\text{H}_3\text{N})\text{-6-R}]$, containing neutral iminopyridine coordinated ligands have been synthesized and fully characterized.

Results and discussion

The aldimino precursors **2a–d** were obtained on a multigram scale with little modifications to the procedures reported in the literature.⁹ All ligands are off-white/pale-yellow solids after extractive work-up and solvent evaporation. Recrystallization from hot MeOH gave the pure compounds as white/pale yellow crystals with melting points ranging from 96 to 123 °C (see Experimental section).

A dark-red THF solution of complex **1** was reacted at room temperature with an equimolar amount of a potentially tridentate iminopyridine ligand (**2b** or **2c**) without any appreciable color change of the starting solution. The reaction mixture was monitored over several hours by ¹H NMR (THF-*d*₈, 293 K) spectroscopy showing only signals from the unreacted starting materials. Solvent evaporation under vacuum gave a dry dark-red solid residue. Dissolving the solid in toluene at room temperature resulted in the immediate change of the solution color from dark-red to brownish-black. After cooling the solution to –20 °C for several days, brownish-black microcrystals of complexes **4** and **5**, suitable for X-ray analysis, separated off. Pure **4** and **5** were obtained from the mother-liquor in 74 and 69% yields, respectively, as poorly soluble compounds in aromatic and aliphatic hydrocarbons (Scheme 2).

Complexes **4** and **5** are moisture- and air-sensitive crystalline solids and their ¹H NMR spectra (C_6D_6 , 293 K) unambiguously accounted for Yb^{II} diamagnetic species with all (rather broadened) signals falling in the 1–8.8 ppm region. The scarce solubility of both complexes in benzene-*d*₆ did not allow to record the corresponding ¹³C{¹H} NMR spectra. On the other hand, the ¹H NMR spectra of both compounds in THF-*d*₈ (293 K) revealed a rapid ligand dissociation, showing the appearance of sharp signals characteristic of **1** and the free IPy ligands (**2b** and **2c**). The UV-VIS spectra of **4** and **5** recorded in *n*-hexane provided evidence of the neutral character of the coordinated IPy ligands (see ESI†).



Scheme 2 Reaction path of **1** with tridentate IPy ligands **2b** and **2c**.

Finally, evidence of the ligands coordination to the ytterbium center was unambiguously provided by X-ray analysis; the X-ray structures of **4** and **5** are shown in Fig. 1 and 2, respectively.

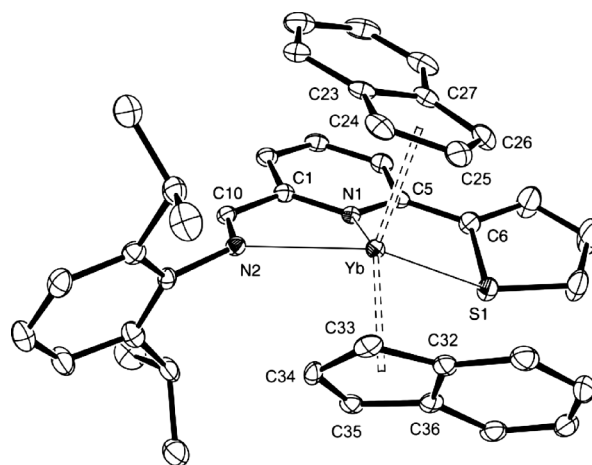


Fig. 1 Crystal structure of $[\text{N}_2^{2\text{Th}}(\text{C}_9\text{H}_6)_2\text{Yb}]\cdot\text{C}_7\text{H}_8$ (**4**). Thermal ellipsoids are drawn at the 40% probability level. Hydrogen atoms and a crystallization toluene molecule are omitted for clarity.

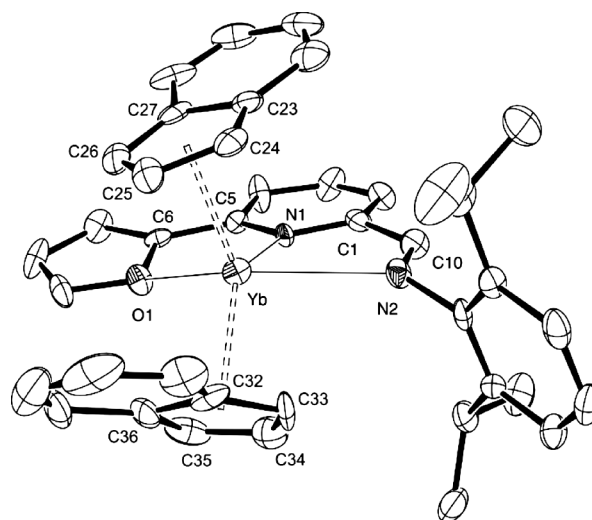


Fig. 2 Crystal structure of $[\text{N}_2^{\text{Fu}}(\text{C}_9\text{H}_6)_2\text{Yb}]$ (**5**). Thermal ellipsoids are drawn at the 40% probability level. Hydrogen atoms are omitted for clarity.

The main structural parameters and a list of selected bond lengths and angles are summarized in Table 1 and Table 2, respectively. Complex **4** crystallizes as a toluene solvate, while crystals of **5** do not contain any crystallization solvent. Both

Table 1 Crystal data and structure refinement for complexes 4–7

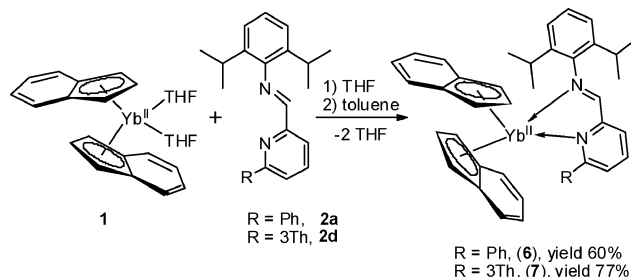
	4	5	6	7
CCDC number	794890	795224	794891	794889
Empirical formula	C ₄₀ H ₃₈ N ₂ SYb·C ₇ H ₈	C ₄₀ H ₃₈ N ₂ OYb	C ₄₂ H ₄₀ N ₂ Yb	C ₄₀ H ₃₈ N ₂ SYb·C ₇ H ₈
<i>M_r</i>	843.96	735.76	745.80	843.96
<i>T</i> /K	100(2)	120(2)	120(2)	100(2)
λ /Å	0.71073	0.71069	0.71069	0.71069
Crystal system	Orthorhombic	Monoclinic	Monoclinic	Orthorhombic
Space group	<i>Pna</i> 2 ₁	<i>Cc</i>	<i>P2</i> ₁ / <i>n</i>	<i>Pna</i> 2 ₁
<i>a</i> /Å	23.6885(7)	10.309(4)	9.293(4)	23.695(9)
<i>b</i> /Å	10.4564(3)	27.522(11)	37.396(1)	10.380(4)
<i>c</i> /Å	15.6524(5)	11.346(5)	10.314(4)	15.684(6)
β /°	90	96.968(3)	114.897(5)	90
<i>V</i> /Å ³	3877.0(2)	3195(2)	3251(2)	3858(3)
<i>Z</i> , <i>D_c</i> /g m ⁻³	4, 1.446	4, 1.529	4, 1.524	4, 1.453
μ /mm ⁻¹	2.501	2.961	2.909	2.514
<i>F</i> (000)	1712	1480	1504	1712
Crystal size/mm	0.50 × 0.40 × 0.30	0.01 × 0.01 × 0.015	0.01 × 0.02 × 0.02	0.08 × 0.10 × 0.15
θ Range for data collection/°	2.13–26	4.20–26.55	4.14–26.46	4.15–28.91
Limiting indices	–29 ≤ <i>h</i> ≤ 29 –12 ≤ <i>k</i> ≤ 12 –19 ≤ <i>l</i> ≤ 19	–12 ≤ <i>h</i> ≤ 11 –33 ≤ <i>k</i> ≤ 33 –14 ≤ <i>l</i> ≤ 12	–10 ≤ <i>h</i> ≤ 11 –46 ≤ <i>k</i> ≤ 42 –12 ≤ <i>l</i> ≤ 12	–28 ≤ <i>h</i> ≤ 32 –13 ≤ <i>k</i> ≤ 13 –21 ≤ <i>l</i> ≤ 20
Reflections collected/unique	31999/7571	15497/5381	24993/5684	15989/7862
Flack parameter	–0.020(5)	0.005(9)	—	–0.013(10)
GOF on <i>F</i> ²	1.067	0.881	0.925	0.953
Data/restraints/parameters	7571/1/465	5381/2/401	5684/0/410	7862/1/425
Final <i>R</i> indices [<i>I</i> > 2 σ (<i>I</i>)]	<i>R</i> ₁ = 0.0184, <i>wR</i> ₂ = 0.0458	<i>R</i> ₁ = 0.0386, <i>wR</i> ₂ = 0.0638	<i>R</i> ₁ = 0.0390, <i>wR</i> ₂ = 0.0669	<i>R</i> ₁ = 0.0321, <i>wR</i> ₂ = 0.0695
<i>R</i> indices (all data)	<i>R</i> ₁ = 0.0190, <i>wR</i> ₂ = 0.0461	<i>R</i> ₁ = 0.0560, <i>wR</i> ₂ = 0.0667	<i>R</i> ₁ = 0.0600, <i>wR</i> ₂ = 0.0703	<i>R</i> ₁ = 0.0431, <i>wR</i> ₂ = 0.0716
$\Delta\rho_{\max, \min}$ /e Å ⁻³	1.41, –0.47	0.975, –0.463	1.283, –0.942	1.214, –0.638

complexes show very similar structures, with the Yb^{II} center adopting a highly distorted trigonal bipyramidal geometry with two η^5 -coordinated indenyl fragments and the tridentate {N,N,S} (4) or {N,N,O} (5) IPy ligands that saturate the metal coordination sphere. The Yb–C_{Cent} distances in 4 (2.475(1) and 2.493(9) Å, Yb–C_{av} = 2.768 Å) and in 5 (2.465(3) and 2.480(4) Å, Yb–C_{av} = 2.749 Å) are slightly longer than those measured in the starting ytterbocene 1 (2.457(1) Å, Yb–C_{av} = 2.73),^{10a,b} and are in line with the values commonly observed in Yb^{II} coordination compounds.^{9c,d} Finally, the shorter distances between the ytterbium center and the three “allylic” carbon atoms of the five-membered rings of each indenyl moiety (C_{24–26} and C_{33–35}) compared to those from the quaternary carbon atoms (C_{23,27} and C_{32,36}), are the proof of a noticeable η^5 -to η^3 -slippage of the indenyl ligands. The α (Cp_{Cent}–Yb–Cp_{Cent}) in 4 and 5 (123.7(9) and 130.66(4)°, respectively) are rather close to the values reported for other divalent Yb^{II} bis(indenyl) compounds.⁹ While Yb^{II}–N distances in 4 have similar values [2.5813(16) and 2.5956(15) Å], the Yb^{II}–N_{imine} distance in 5 is markedly longer [2.714(6) Å] than that measured between the metal center and the pyridine nitrogen atom [2.527(10) Å]. Overall, the Yb^{II}–N coordination bond lengths in 4 and 5 are close to those formerly reported in the literature for eight- and nine-coordinated Yb^{II} derivatives,^{11,5d} while they appear significantly longer compared to those measured in Yb^{III} species coordinated by a radical-anionic N,N-bidentate IPy ligand [2.326(3), 2.352(3) Å];^{8a} the Yb^{II}–N bond lengths are also markedly longer than the Yb^{III}–N distances in eight-coordinate complexes bearing neutral 2,2′-bipyridyl or 1,10-phenanthroline ligands (2.37, 2.36 Å).¹² While no Yb^{II} compounds containing a sulfur donor atom like 4 have been reported in the literature so far (which does not allow the authors to make any direct comparison of the Yb^{II}–S bond length with related Yb^{II}–S distances), the Yb^{II}–O distance in 5 [2.592(5) Å] is significantly

longer than that measured in the known nine-coordinate Yb^{II} complex (C₉H₆CH₂C₅H₄N)₂Yb(OC₄H₈) [2.449(5) Å].^{10b} Finally, the N(2)–C(10) bond lengths [1.282(3) Å, 4; 1.281(9) Å, 5] are typical of C≡N double bonds and the dihedral angles θ [N(1)–C(1)–C(10)–N(2)] are very close to those measured in *d*-transition-metal complexes stabilized by neutral *N,N*-iminopyridine systems (Table 2).¹³

In agreement with the results of solid-state investigations, magnetic measurements conducted on 4 and 5 evidenced the diamagnetic character of the two complexes within the 2–300 K temperature range and thus the closed shell configuration of both Yb and ligand.

Studying the reaction of 1 with an equimolar amount of the bidentate IPy ligands (2a and 2d) under similar experimental conditions to those described above (Scheme 3), gave air- and moisture-sensitive brownish-black microcrystals of complexes 6 and 7 in 60 and 77% yield, respectively.

**Scheme 3** Reaction path of 1 with bidentate iminopyridine ligands 2a and 2d.

Both compounds showed scarce solubility in aromatic and aliphatic hydrocarbons, thus hampering the characterization of

Table 2 Selected bond distances (Å) and angles (°) for complexes **4–7**. See ESI† for a complete list of the crystallographic parameters

	4	5	6	7
Yb–N1	2.5813(16)	2.527(10)	2.592(4)	2.538(4)
Yb–N2	2.5956(15)	2.714(6)	2.597(4)	2.591(4)
Yb–S1	3.002(5)	—	—	—
Yb–O1	—	2.592(5)	—	—
Yb–C23	2.814(2)	2.791(7)	—	2.846(5)
Yb–C24	2.691(2)	2.701(7)	—	2.722(5)
Yb–C25	2.682(2)	2.701(12)	2.773(4)	2.688(4)
Yb–C26	2.748(2)	2.719(12)	2.696(4)	2.751(5)
Yb–C27	2.853(2)	2.810(7)	2.722(5)	2.872(5)
Yb–C28	—	—	2.796(5)	—
Yb–C29	—	—	2.853(5)	—
Yb–C32	2.8457(19)	2.800(7)	—	2.850(5)
Yb–C33	2.729(2)	2.672(12)	—	2.752(5)
Yb–C34	2.6905(15)	2.689(9)	2.829(5)	2.673(5)
Yb–C35	2.7484(19)	2.754(8)	2.751(5)	2.690(5)
Yb–C36	2.876(2)	2.860(7)	2.699(5)	2.817(6)
Yb–C37	—	—	2.703(5)	—
Yb–C38	—	—	2.802(5)	—
N2–C10	1.282(3)	1.281(9)	1.276(6)	1.289(6)
N1–Yb–N2	66.55(5)	64.8(2)	65.27(12)	67.11(13)
N1–Yb–S1	63.00(4)	—	—	—
N1–Yb–O1	—	62.9(2)	—	—
Yb–Cp _{Cent}	2.475(1)	2.465(3)	2.473(2)	2.473(3)
Yb–Cp _{Cent}	2.493(9)	2.480(4)	2.487(2)	2.490(2)
Cp _{Cent} –Yb–Cp _{Cent}	123.7(9)	130.66(4)	117.3(2)	124.4(2)
N1–C5–C6–S1	16.8(2)	—	—	—
N1–C5–C6–O1	—	–12.6(9)	—	—
N1–C5–C6–C7	—	—	–37.5(7)	23.8(7)
N1–C1–C10–N2	11.0(3)	–5.1(3)	—	12.2(7)
N1–C1–C12–N2	—	—	–10.4(7)	—

6 in solution. The ¹H NMR and UV-VIS spectra (see ESI†) of **7** were still consistent with a divalent oxidation state of the ytterbium atom and with a neutral coordinated iminopyridine ligand.

Once again, clear evidence of the IPy ligands coordination mode to the ytterbium center was unambiguously provided by the X-ray analysis of both complexes, whose X-ray structures are shown in Fig. 3 and 4, respectively.

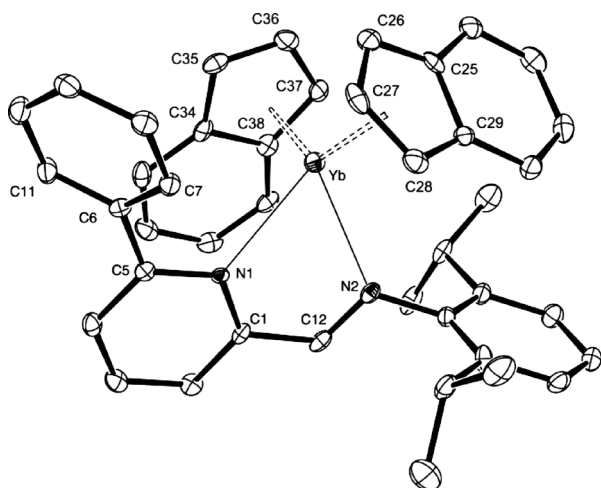


Fig. 3 Crystal structure of $[\text{N}_2^{3\text{H}}(\text{C}_9\text{H}_6)_2\text{Yb}]$ (**6**). Thermal ellipsoids are drawn at the 40% probability level. Hydrogen atoms are omitted for clarity.

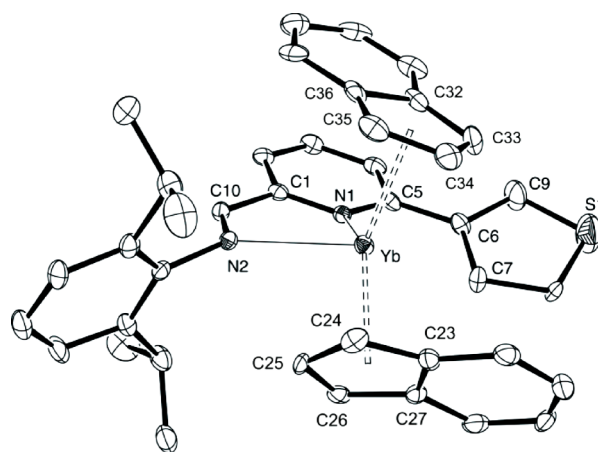


Fig. 4 Crystal structure of $[\text{N}_2^{3\text{H}}(\text{C}_9\text{H}_6)_2\text{Yb}] \cdot \text{C}_7\text{H}_8$ (**7**). Thermal ellipsoids are drawn at the 40% probability level. Hydrogen atoms and a crystallization toluene molecule are omitted for clarity.

Table 1 lists all the crystal and structural refinement data, while selected bond lengths and angles for **6** and **7** are summarized in Table 2. Similarly to above, complex **7** crystallizes as a toluene solvate, while the crystals of **6** do not contain any additional crystallization solvent. Interestingly, the thiophene-containing isomers **4** and **7** are isostructural; the different orientation of the sulfur atom in the heterocyclic substituent does not seem to influence the crystal packing of the resulting complexes. Despite in **7** the S atom is bent away from the metal centre, it is not involved in any intermolecular interaction with the neighbouring molecules in the lattice. The $\theta[\text{N}(1)\text{--C}(5)\text{--C}(6)\text{--S}(1)]$ and $\theta[\text{N}(1)\text{--C}(5)\text{--C}(6)\text{--C}(7)]$ dihedral angles in **4** and **7** are also similar [16.8(2) and 23.8(7)°, respectively], this confirming the analogous orientation of the heterocyclic ring in the two compounds. Unlike **4** and **5**, the X-ray diffraction analyses of **6** and **7** (Fig. 3 and 4) revealed that the metal centers were four-coordinated, with two indenyl fragments and a bidentate {N,N} iminopyridine ligand completing the metal coordination sphere. Overall, both structures showed distorted tetrahedral coordination geometries. As expected, the sulfur atom of the regioisomeric **2d** ligand in complex **7**, did not take part into any intra- or intermolecular coordination, being oriented away from the metal center.

The average Yb–C_{av} bond distances [2.763 Å (**6**) and 2.766 Å (**7**)] are very close to those measured in **4** and **5**, suggesting a partial slippage of the indenyl fragments (possible η^3 - instead of the expected η^5 -coordination). The Yb–N bond distances in **6** [2.592(4), 2.597(4) Å] and **7** [2.538(4), 2.591(4) Å] are also similar to those measured in **4** and **5**, with values in the typical range for the related Yb^{II} coordination compounds containing neutral N-ligands.^{11,5d} Finally, the dihedral angles $\theta[\text{N}(1)\text{--C}(1)\text{--C}(12)\text{--N}(2)]$ in **6** and $\theta[\text{N}(1)\text{--C}(1)\text{--C}(10)\text{--N}(2)]$ in **7** are again very close to those reported for other similar Yb-coordination complexes¹² and *d*-transition-metal complexes stabilized by neutral N,N-iminopyridine systems.¹³

Magnetic measurements conducted on **6** and **7** showed that both systems (in the solid state) are essentially diamagnetic (with the exception of a weak and unavoidable paramagnetic impurity) up to 240 K (Fig. 5). However, starting from 245 K for **6** and 260 K for **7**, the χT product clearly began to increase for both

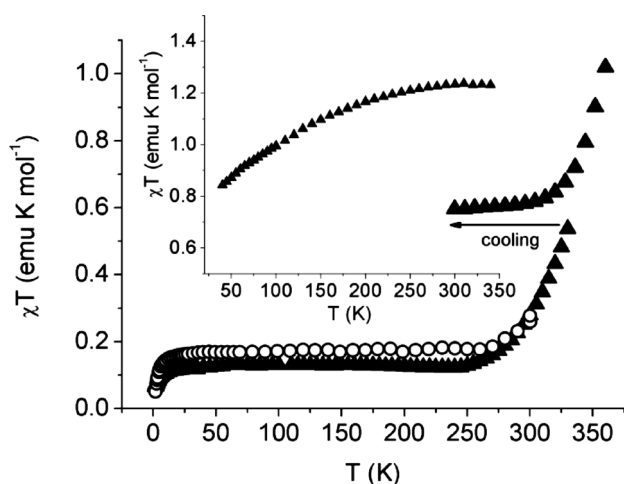


Fig. 5 Magnetic susceptibility data (χT vs. T) for **6** (empty circles) and **7** (full triangles); for the latter a second heating cycle after cooling back to 240 K is reported. The inset shows the χT vs. T plot for complex **7** measured after several heating/cooling cycles between 240 and 340 K.

samples, suggesting the possible occurrence of a temperature-induced intramolecular electron transfer¹⁴ between the rare-earth metal center and the ligand framework.¹⁵ This should lead to an Yb^{III}-radical configuration for which a high temperature χT value of 2.95 emu K mol⁻¹ is expected.¹⁶ Test measurements performed only on **7** showed that the transition is not reverted upon cooling back the sample to 240 K, since it maintains its high temperature magnetic susceptibility. The repetition of this procedure led to a complete disruption of the complex molecular structure, as evidenced by the χT vs. T plot (see inset on Fig. 5). The observed decrease in χT vs. T in the transformed compound is in agreement with the presence of a substantial fraction of Yb^{III}, since it can be ascribed to the progressive depopulation of Stark sublevels of ²F_{7/2} ground state of Yb^{III}.

Notably, the occurrence of an intramolecular electron transfer process is not in contrast with the data obtained by the X-ray and NMR analyses, which indicated the diamagnetic nature of both samples. Indeed, crystallographic data were collected at 120 K, a temperature at which the magnetic measurements confirmed the diamagnetic character of both complexes. As for NMR results, the fact that no diamagnetic-paramagnetic transition was observed at room temperature simply indicates that the solution and the solid-state behavior are different. This is not surprising, since it is well known that both the aggregation state and the local environment around the molecule are of paramount importance in determining the temperature at which intramolecular electron transfer processes take place.¹⁷

All the collected experimental data unambiguously indicate that ligands **2a–d** take part to the ytterbium coordination sphere as either tridentate {N,N,S and N,N,O} or bidentate {N,N} neutral ligands,¹⁸ to afford exclusively divalent Yb^{II} diamagnetic compounds.

The introduction of a (coordinating or non-coordinating) aryl substituent on the sixth position of the pyridine ring changes the **1**/IPy ligand reaction outcome significantly. In order to get additional experimental feedback on this aspect, the electrochemical behavior of the four IPys **2a–d** has been investigated and compared with that of the unsubstituted ligand **2e**. Cyclic voltammetry (CV)

experiments were recorded on a 5 mM ligand solution in dry and degassed DMF (5 mL) using ^tBu₄N⁺BF₄⁻ (0.1 M) as conductivity buffer.

The CV profiles of all ligands, together with the relative peak and half-wave potential values (referred to the FeCp₂/FeCp₂⁺ redox couple) are reported in Fig. 6. For all the scrutinized ligands, the higher the potential scan rate the lower the peak reduction potential value, which accounts for a slow electron transfer process. All CVs showed highly asymmetric profiles, with the reverse peak current values (oxidation) always lower than the forward one (reduction). Except for **2d**, all electron transfers are chemically reversible and electrochemically quasi-reversible. From the analysis of the CV profiles, one may conclude that all aryl-substituted iminopyridine ligands (**2a–d**) present similar electron accepting properties and peak shapes with very similar reduction potential values (imino vs. amine). In contrast to the observed reactivity with **1**,^{8a} the unsubstituted IPy system **2e** showed the lowest tendency to stabilize negative extra charges because of its lower reduction potential value (V_p) and the reduced extension of its conjugated network [compared with the other IPy systems (**2a–d**)].

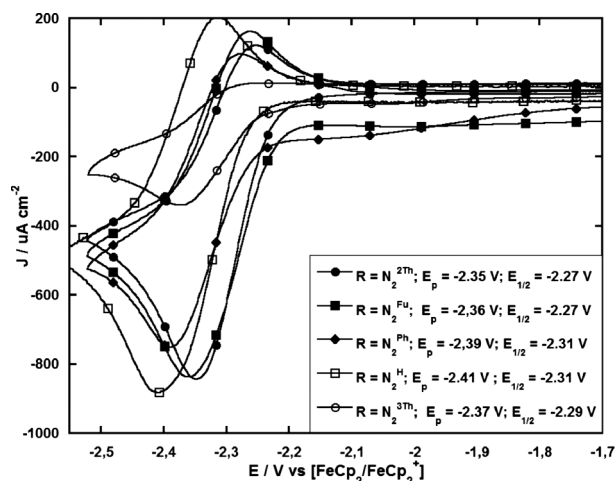


Fig. 6 Cyclic voltammograms of the ligands **1a–e**. CV curves were acquired in anhydrous DMF using tetraethyl ammonium tetrafluoroborate (0.1 M) as conductivity buffer. Scan rate: 50 mV s⁻¹, sample concentration: 5 mM.

The presence of additional Lewis basic sites in the ligands **2b** and **2c** (both ligands able to participate as tridentate systems) results in a more rigidly coordinated IPy framework and the formation of Yb^{II} complexes with increased coordination numbers. In spite of that, only negligible electronic factors have to be considered while comparing the reactivity of **1** with 6-aryl substituted IPys (**2a–d**) and **2e**. Indeed, neither the imine reduction potential values for **2a–d** nor their coordination ability [bidentate (**2a, d**) vs. tridentate (**2b, c**)] can be reasonably invoked to justify the different pathways observed in the reaction of **1** with 6-aryl substituted (**2a–d**) and unsubstituted (**2e**) IPy ligands, respectively. In particular, the reactivity observed with the regioisomeric ligands **2b** and **2d**, definitively ruled out any electronic influence or coordination effect of the aromatic moiety at the pyridine unit on the reaction path. Thus, simple steric contributions resulting from the presence of bulky aryl substituents on the 6-position of the pyridine ring

have to be considered as responsible for the modulation of the ytterbium redox chemistry. As a result, sterically crowded IPy ligands **2a–d** react with **1** leading to the formation of simple Yb^{II} coordination adducts as a result of a THF/ligand exchange at the metal center. Neither evidence for Yb^{II}/Yb^{III} oxidation nor ligand modification (as reported for **2e**) have been observed.

Conclusions

In conclusion, we have described a steric control on the redox properties of ytterbocene **1** by bidentate {N,N} and tridentate {N,N,S or N,N,O} iminopyridine ligands (IPys) variably substituted on the 6-position of the pyridine ring. In contrast to the unprecedented reactivity of the unsubstituted IPy **2e** with ytterbocene **1**,^{8a} the reaction of **1** with ligands **2a–d** simply occurs by the replacement of the two coordinated THF molecules with one bi- or tri-dentate IPy ligand, with retention of ytterbium oxidation state. While the presence of additional coordinating basic sites on the IPy ligands (S or O donor atoms) results in more rigidly coordinated systems and higher metal coordination numbers, neither significant electronic effects (**4** vs. **7**) nor different ligand electron accepting properties (Fig. 6) can be reasonably invoked to justify the observed reactivity (**1/2a–d** vs. **1/2e**).

Magnetic measurements conducted on the solid samples (**4–7**) unambiguously showed the diamagnetic character of all complexes below 240 K with the occurrence of an intramolecular electron transfer process taking place only for **6** and **7** at higher temperature (over 240 K). This indicates a higher stability of the diamagnetic electronic configuration (closed shell) for the complexes containing tridentate IPy ligands vs. bidentate ones. Finally, the reactivity described in this paper represents a new example of steric control of the redox chemistry of (η⁵-C₉H₇)₂Yb^{II}(THF)₂ towards iminopyridines.

Experimental

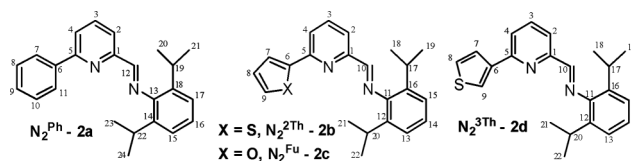
General remarks

All air- and/or moisture-sensitive reactions were performed under either nitrogen or argon in flame-dried flasks using standard Schlenk-type techniques or in a dry-box filled with nitrogen. After drying over KOH, THF was purified by distillation from sodium/benzophenone ketyl. Hexane and toluene were dried over sodium/triglyme benzophenone ketyl and distilled prior to use. Indene was purchased from Acros and ytterbocene (C₉H₇)₂Yb(THF)₂ was prepared according to literature procedure.^{5c} All the other reagents and solvents were used (otherwise stated) as purchased from commercial suppliers. ¹H and ¹³C{¹H} NMR spectra were recorded on either a Bruker DPX 200 (200.13 and 50.32 MHz, respectively) or a Bruker Avance DRX-400 (400.13 and 100.62 MHz, respectively). Chemical shifts are reported in ppm (δ) relative to TMS, referenced to the chemical shifts of residual solvent resonances (¹H and ¹³C). IR spectra were recorded as Nujol mulls on a "Bruker-Vertex 70" spectrophotometer. Magnetic susceptibility data were collected with a Quantum Design MPMS-XL SQUID magnetometer working in the temperature range of 1.8–300 K (extended to 340 K for measurements on **7**) and the magnetic field range up to 5 Tesla. Samples were prepared in glove-box by wrapping them

in Teflon tape and quickly transferred to the SQUID vacuum chamber. The data were corrected for the intrinsic diamagnetism of the sample, calculated from the Pascal's constants¹⁹ and sample holder contribution, measured in the same field and temperature range.

Lanthanide metal analyses were carried out by complexometric titration. The C, H elemental analysis was carried out in the microanalytical laboratory of IOMC or at ICCOM by means of a Carlo Erba Model 1106 elemental analyzer with an accepted tolerance of ±0.4 units on carbon (C), hydrogen (H) and nitrogen (N). Melting points were ensued by using a Stuart Scientific Melting Point apparatus SMP3. CV experiments were performed on a PARSTAT 2773 galvanostat/potentiostat (Princeton Applied Research) equipped with Dr Bob's Cell(tm) (Gamry) using the classical three electrode topology; the Ag|AgCl|KCl_{sat} (Gamry) reference electrode, a 3 mm diameter glassy carbon as working electrode and a platinum wire as counter electrode. All solutions were prepared in glove box under inert atmosphere (N₂), and the cell was well purged with N₂ prior to use. The potential was varied between -1.0 and -2.0 V (vs. Ag|AgCl|KCl_{sat}) at potential sweep rates of 10, 20, 50, 100, 200 and 400 mV s⁻¹ in cathodic direction. After the measurement on each ligand, a solution of 5 mM ferrocene in the same conditions was measured to calibrate the potential; all potentials were finally referred to the FeCp₂/FeCp₂⁺ redox couple.

Ligands **2a–e** were prepared on a multigram scale with little variation to literature procedure.²⁰ In particular, ligands **2a–d** were obtained using aldiminopyridinate derivatives instead of ketoimino ones (for ligand **2a–c** see refs. 9a,b and 21; for ligand **2d** see ref. 9b). Ligand **2e** was prepared according to literature procedures.²²



Ligands **2a–d** were isolated as microcrystalline solids by cooling methanol solutions to 4 °C overnight [**2a**: 74% yield, yellow microcrystals; mp 96 °C. IR (KBr): $\nu_{\text{C=N}}$ 1648 cm⁻¹. MS *m/z* (%): 342 (M⁺, 76); 377 (M⁺ + 1, 19); 327 (M⁺ - 15, 100). ¹H NMR (300 MHz, CD₂Cl₂, 293 K): δ 1.21 (d, ³J_{HH} = 6.8 Hz, 12H, CH(CH₃), H^{20,21,23,24}), 3.03 (sept, ³J_{HH} = 6.8 Hz, 2H, CH(CH₃), H^{19,22}), 7.12–7.23 (3H, CH Ar, H^{15,16,17}), 7.45–7.57 (3H, CH Ar, H^{8,9,10}), 7.92 (dd, ³J_{HH} = 7.8 Hz, 1H, CH Ar, H²), 7.97 (pt, ³J_{HH} = 7.8 Hz, 1H, CH Ar, H³), 8.11–8.15 (2H, CH Ar, H^{7,11}), 8.26 (dd, ³J_{HH} = 7.8 Hz, 1H, CH Ar, H⁴), 8.41 (s, 1H, CHN, H¹²). ¹³C{¹H} NMR (75 MHz, CD₂Cl₂, 293 K): δ 23.1 (CH(CH₃)₂, C^{20,21,23,24}), 27.9 (CH(CH₃)₂, C^{19,22}), 119.3 (C⁴), 121.8 (C²), 122.9 (C^{15,17}), 124.3 (C¹⁶), 126.8 (C^{7,11}), 128.7 (C^{8,10}), 129.2 (C⁹), 137.2 (C^{14,18}), 137.4 (C³), 138.7 (C⁶), 148.6 (C¹³), 154.3 (C¹), 157.0 (C⁵), 163.6 (C¹²). Anal. Calc. (%) for C₂₄H₂₆N₂ (342.48): C, 84.17; H, 7.65; N, 8.18. Found: C, 84.21; H, 7.43; N, 8.01%. **2b**: 95% yield, yellow crystals; mp 123 °C. IR (KBr): $\nu_{\text{C=N}}$ 1646 cm⁻¹. MS *m/z* (%): 378 (M⁺, 76); 379 (M⁺ + 1, 20); 333 (M⁺ - 15, 100). ¹H NMR (300 MHz, CD₂Cl₂, 293 K): δ 1.17 (d, ³J_{HH} = 6.8 Hz, 12H, CH(CH₃), H^{18,19,21,22}), 2.97 (sept, ³J_{HH} = 6.8 Hz, 2H, CH(CH₃), H^{17,20}), 7.08–7.19 (4H, CH Ar, H^{8,13,14,15}), 7.43 (dd, ³J_{HH} = 5.05 Hz, ⁴J_{HH} = 1.14 Hz, 1H, CH Ar, H⁷), 7.68 (dd, ³J_{HH} = 3.69 Hz, ⁴J_{HH} = 1.14 Hz, 1H, CH Ar, H⁹),

7.78 (dd, $^3J_{\text{HH}} = 7.8$ Hz, $^4J_{\text{HH}} = 1.11$ Hz, 1H, CH Ar, H²), 7.84 (t, $^3J_{\text{HH}} = 7.8$ Hz, 1H, CH Ar, H³), 8.14 (dd, $^3J_{\text{HH}} = 7.8$ Hz, $^4J_{\text{HH}} = 1.11$ Hz, 1H CH Ar, H⁴), 8.29 (s, 1H, CHN, H¹⁰). $^{13}\text{C}\{^1\text{H}\}$ NMR (75 MHz, CD_2Cl_2 , 293 K): δ 23.1 (CH(CH₃)₂, C^{18,19,21,22}), 27.9 (CH(CH₃)₂, C^{17,20}), 119.0 (C⁴), 120.2 (C²), 122.9 (C^{13,15}), 124.3 (C¹⁴), 125.0 (C⁹), 127.8 (C⁷), 128.0 (C⁸), 137.1 (C^{12,16}), 137.3 (C³), 144.2 (C⁶), 148.6 (C¹¹), 152.4 (C¹), 154.2 (C⁵), 163.1 (C¹⁰). Anal. Calc. (%) for C₂₂H₂₄N₂S (348.51): C, 75.82; H, 6.94; N, 8.04. Found: C, 76.01; H, 6.83; N, 7.87%. **2c**: 88% yield, yellow crystals; mp 110 °C. IR (KBr): $\nu_{\text{C=N}}$ 1637 cm⁻¹. MS m/z (%): 332 (M⁺, 56); 317 (M⁺ - 15, 77); 146 (100). ^1H NMR (300 MHz, CD_2Cl_2 , 293 K): δ 1.10 (d, $^3J_{\text{HH}} = 6.8$ Hz, 12H, CH(CH₃), H^{18,19,21,22}), 2.90 (sept, $^3J_{\text{HH}} = 6.8$ Hz, 2H, CH(CH₃), H^{17,20}), 6.51 (dd, $^3J_{\text{HH}} = 3.4$ Hz, $^4J_{\text{HH}} = 1.8$ Hz, 1H, CH Ar, H⁸), 7.02–7.12 (4H, CH Ar, H^{7,13,14,15}), 7.52 (m, 1H, CH Ar, H⁹), 7.73 (dd, $^3J_{\text{HH}} = 7.8$ Hz, $^4J_{\text{HH}} = 1.14$ Hz, 1H, CH Ar, H²), 7.82 (pt, $^3J_{\text{HH}} = 7.8$ Hz, 1H, CH Ar, H³), 8.08 (dd, $^3J_{\text{HH}} = 7.8$ Hz, $^4J_{\text{HH}} = 1.11$ Hz, 1H CH Ar, H⁴), 8.23 (s, 1H, CHN, H¹⁰). $^{13}\text{C}\{^1\text{H}\}$ NMR (75 MHz, CD_2Cl_2 , 293 K): δ 23.1 (CH(CH₃)₂, C^{18,19,21,22}), 27.8 (CH(CH₃)₂, C^{17,20}), 109.0 (C⁷), 112.0 (C⁸), 119.1 (C⁴), 119.8 (C²), 122.9 (C^{13,15}), 124.3 (C¹⁴), 137.1 (C^{12,16}), 137.3 (C³), 143.5 (C⁹), 148.5 (C¹¹), 149.2 (C¹¹), 153.3 (C¹), 154.2 (C⁵), 163.2 (C¹⁰). Anal. Calc. (%) for C₂₂H₂₄N₂O (332.45): C, 79.48; H, 7.28; N, 8.43. Found: C, 73.19; H, 7.21; N, 8.40%. **2d**: 96% yield, yellow crystals; mp 99 °C. IR (KBr): $\nu_{\text{C=N}}$ 1646 cm⁻¹. MS m/z (%): 348 (M⁺, 77); 349 (M⁺ + 1, 20); 333 (M⁺ - 15, 100). ^1H NMR (300 MHz, CD_2Cl_2 , 293 K): δ 1.20 (d, $^3J_{\text{HH}} = 6.8$ Hz, 12H, CH(CH₃), H^{18,19,21,22}), 3.01 (sept, $^3J_{\text{HH}} = 6.8$ Hz, 2H, CH(CH₃), H^{17,20}), 7.11–7.22 (3H, CH Ar, H^{13,14,15}), 7.47 (dd, $^3J_{\text{HH}} = 5.0$ Hz, $^4J_{\text{HH}} = 3.0$ Hz, 1H, CH Ar, H⁷), 7.77–7.80 (2H, CH Ar, H^{2,8}), 7.92 (pt, $^3J_{\text{HH}} = 7.7$ Hz, 1H, CH Ar, H³), 8.04 (dd, $^4J_{\text{HH}} = 3.0$ Hz, $^4J_{\text{HH}} = 1.2$ Hz, 1H CH Ar, H⁹), 8.20 (dd, $^3J_{\text{HH}} = 7.7$ Hz, $^4J_{\text{HH}} = 1.0$ Hz, 1H, CH Ar, H⁴) 8.35 (s, 1H, CHN, H¹⁰). $^{13}\text{C}\{^1\text{H}\}$ NMR (75 MHz, CD_2Cl_2 , 293 K): δ 23.1 (CH(CH₃)₂, C^{18,19,21,22}), 27.9 (CH(CH₃)₂, C^{17,20}), 119.0 (C⁴), 121.6 (C²), 122.9 (C^{13,15}), 123.9 (C⁹), 124.3 (C¹⁴), 126.2 (C⁸), 126.4 (C⁷), 137.2 (C^{12,16}), 137.3 (C³), 144.7 (C⁶), 148.6 (C¹¹), 153.2 (C¹), 154.2 (C⁵), 163.6 (C¹⁰). Anal. Calc. (%) for C₂₂H₂₄N₂S (348.51): C, 75.82; H, 6.94; N, 8.04. Found: C, 75.75; H, 6.90; N, 7.91%.

General procedure for the synthesis of ($\eta^5\text{-C}_9\text{H}_7$)₂Yb{[1-(6-organylpiperidin-2-yl)methylidene](2,6-diisopropylphenyl)amine} (4–7)

In a typical procedure, a THF solution (10 mL) of **1** (0.50 g, 0.91 mmol) was treated dropwise with a THF solution (10 mL) of the appropriate ligand (**2a–d**) (0.91 mmol) and the reaction mixture was heated at 50 °C for 0.5 h. Afterwards, solvent was removed under reduced pressure and the solid residue was dissolved in toluene (20 mL). The resulting solution was then heated at 50 °C for a further 0.5 h before cooling it to -20 °C overnight. **4**: 74% yield, brownish-black crystals; IR (Nujol, KBr, cm⁻¹): 3067 (w), 1642 (s), 1583 (m), 1310 (m), 1250 (m), 1167 (m), 1035 (m), 802 (s), 770 (s), 750 (s), 742 (s), 648 (s), 623 (m), 495 (s), 439 (s). ^1H NMR (400 MHz, C₆D₆, 293 K): δ 1.13 (d, $^3J_{\text{HH}} = 7.26$ Hz, 12 H, CH(CH₃)), 3.12 (br s, 2 H, CH(CH₃)), 5.49 (br s, 1 H, Ar), 5.93 (br s, 2 H, Ar), 6.23 (s, 2 H, Ar), 6.72 (s, 3 H, Ar), 6.76 (s, 4 H, Ar), 6.99–7.05 (m, 4 H, Ar), 7.26–7.33 (m, 4 H, Ar), 8.14–8.48 (m, 4 H, Ar + N=CH). Anal. Calc. for C₄₇H₄₆N₂SYb: C 66.88, H 5.49, Yb 20.49. Found: C 66.39, H 5.12, Yb 20.77%. **5**: 69% yield, brownish-black crystals; IR (Nujol, KBr, cm⁻¹): 3064 (w), 1640

(s), 1585 (m), 1325 (m), 1167 (m), 1035 (m) 930 (m), 860 (m), 802 (s), 748 (s), 730 (s), 600 (m), 480 (s), 430 (s). ^1H NMR (400 MHz, C₆D₆, 293 K): δ 1.18 (d, $^3J_{\text{HH}} = 6.77$ Hz, 12 H, CH(CH₃)), 3.12 (br s, 2 H, CH(CH₃)), 5.75 (br s, 2 H, Ar), 6.23 (br s, 2 H, Ar), 6.72 (br s, 2 H, Ar), 6.90 (m, 2 H, Ar), 7.04 (s, 2 H, Ar), 7.09–7.13 (m, 4 H, Ar), 7.26–7.33 (m, 4 H, Ar), 7.62–7.69 (m, 2 H, Ar), 8.20–8.57 (m, 4 H, Ar + N=CH). Anal. Calc. for C₄₀H₃₈N₂OYb: C 65.29, H 5.16, Yb 23.51. Found: C 64.87, H 5.00, Yb 23.60%. **6**: 60% yield, brownish-black crystals; IR (Nujol, KBr, cm⁻¹): 3060 (w), 1642 (m), 1583 (m), 1310 (m), 1250 (m), 1210 (m), 1167 (m), 1100 (m), 980 (m), 850 (m), 820 (m), 742 (s), 726 (s), 690 (s), 623 (m), 530 (m). Anal. Calc. for C₄₂H₄₀N₂Yb: C 67.64, H 5.40, Yb 23.20. Found: C 67.20, H 5.00, Yb 23.49%. **7**: 77% yield, brownish-black crystals; IR (Nujol, KBr, cm⁻¹): 3060 (w), 1642 (s), 1583 (s), 1570 (s), 1324 (m), 1250 (m), 1167 (m), 1035 (m), 990 (m), 972 (m), 960 (m), 824 (m), 802 (s), 764 (s), 742 (s), 726 (s), 643 (m), 530 (m), 450 (s), 425 (s). ^1H NMR (400 MHz, C₆D₆, 293 K): δ 1.17 (br s, 12 H, CH(CH₃)), 3.20 (br s, 2 H, CH(CH₃)), 5.00 (s, 1 H, Ar), 5.54 (s, 2 H, Ar), 5.84 (s, 2 H, Ar), 6.23 (s, 1 H, Ar), 6.48 (s, 1 H, Ar), 6.85 (br s, 4 H, Ar), 7.04 (br s, 2 H, Ar), 7.26 (br s, 4 H, Ar), 7.55 (s, 5 H, Ar), 8.39–8.57 (m, 2 H, Ar + N=CH). Anal. Calc. for C₄₇H₄₆N₂SYb: C 66.88, H 5.49, Yb 20.49. Found: C 66.43, H 5.07, Yb 20.60.

X-Ray crystallography

The data for complex **4** were collected on a SMART APEX diffractometer [graphite-monochromated, Mo-K α radiation ($\lambda = 0.71073$ Å), ω - and θ -scan technique], while those for complexes **5–7** were collected on an Oxford Diffraction XCALIBUR 3 diffractometer equipped with a CCD area detector, with Mo-K α radiation. The absorption correction was applied with the program ABSPACK 1.17.²³ Direct methods implemented in Sir97²⁴ were used to solve the structures and the refinements were performed by full-matrix least-squares against F^2 implemented in SHELX97.²⁵ All the non-hydrogen atoms were refined anisotropically, while the hydrogen atoms were fixed in calculated positions and refined isotropically with the thermal factor depending on the one of the atom to which they are bound. The geometrical calculations were performed by PARST97²⁶ and molecular plots were produced by the program ORTEP3.²⁷ Crystallographic data and structure refinement details are given in Table 1.

Acknowledgements

This work was supported by the Russian Foundation for Basic Research and the Government of Nizhny Novgorod region (grant No. 09-03-97018-p), The Ministry of Education and Science (state contract No. II 1106 26.08.2009), Program of the Presidium of the Russian Academy of Science (RAS), and RAS Chemistry and Material Science Division. A. A. T. and G. G. also thank the GDRE project for financial support.

Notes and references

- 1 G. van Koten and K. Vrieze, *Adv. Organomet. Chem.*, 1982, **21**, 151–239.
- 2 (a) F. G. N. Cloke, H. C. de Lemos and A. A. Sameh, *J. Chem. Soc., Chem. Commun.*, 1986, 1344–1345; (b) F. G. N. Cloke, *Chem. Soc. Rev.*, 1993, **22**, 17–21; (c) A. Recknagel, M. Noltemeyer and F. T. Edelmann, *J. Organomet. Chem.*, 1991, **410**, 53–61; (d) A. Scholz, K.-H. Thiele,

- J. Scholz and R. Weimann, *J. Organomet. Chem.*, 1995, **501**, 195–200; (e) P. Poremba and F. T. Edlmann, *J. Organomet. Chem.*, 1997, **549**, 101–104; (f) H. Goerls, B. Neumueller, A. Scholz and J. Scholz, *Angew. Chem.*, 1995, **107**, 372–375; H. Goerls, B. Neumueller, A. Scholz and J. Scholz, *Angew. Chem., Int. Ed. Engl.*, 1995, **34**, 673–676; (g) J. Scholz, H. Goerls, H. Schumann and R. Weimann, *Organometallics*, 2001, **20**, 4394–4402.
- 3 (a) A. A. Trifonov, *Eur. J. Inorg. Chem.*, 2007, 3151–3167; (b) M. D. Walter, D. J. Berg and R. A. Andersen, *Organometallics*, 2007, **26**, 2296–2307; (c) P. Cui, Y. Chen, G. Wang, G. Li and W. Xia, *Organometallics*, 2008, **27**, 4013–4016; (d) K. Vasudevan and A. H. Cowley, *Chem. Commun.*, 2007, 3464–3466.
- 4 $\text{Yb}^{\text{II}}-\text{Yb}^{\text{III}}$ reduction potential in aqueous solution vs. SHE: -1.15 V. For a comparison with other lanthanide $\text{M}^{\text{II}}-\text{M}^{\text{III}}$ reduction potentials, see also: (a) L. R. Morss, *Chem. Rev.*, 1976, **76**, 827–841; (b) R. G. Finke, S. R. Keenan, D. A. Shirardi and P. L. Watson, *Organometallics*, 1986, **5**, 598–601; (c) A. M. Bond, G. B. Deacon and R. H. Newnham, *Organometallics*, 1986, **5**, 2312–2316.
- 5 (a) A. A. Trifonov, E. N. Kirillov, M. N. Bochkarev, H. Schumann and S. Muehle, *Russ. Chem. Bull.*, 1999, **48**, 382–384; (b) A. A. Trifonov, Yu. A. Kurskii, M. N. Bochkarev, S. Muehle, S. Dechert and H. H. Schumann, *Russ. Chem. Bull.*, 2003, **52**, 601–606; (c) A. A. Trifonov, E. A. Fedorova, V. N. Ikorskii, S. Dechert, H. Schumann and M. N. Bochkarev, *Eur. J. Inorg. Chem.*, 2005, 2812–2818; (d) A. A. Trifonov, E. A. Fedorova, G. K. Fukin, V. N. Ikorskii, Yu. A. Kurskii, S. Dechert, H. Schumann and M. N. Bochkarev, *Russ. Chem. Bull.*, 2004, **53**, 2736–2743.
- 6 (a) A. A. Trifonov, E. A. Fedorova, G. K. Fukin, N. O. Druzhkov and M. N. Bochkarev, *Angew. Chem., Int. Ed.*, 2004, **43**, 5045–5048; (b) A. A. Trifonov, E. A. Fedorova, G. K. Fukin, E. V. Baranov, N. O. Druzhkov and M. N. Bochkarev, *Chem.–Eur. J.*, 2006, **12**, 2752–2757.
- 7 A. A. Trifonov, I. A. Borovkov, E. A. Fedorova, G. K. Fukin, J. Larionova, N. O. Druzhkov and V. K. Cherkasov, *Chem.–Eur. J.*, 2007, **13**, 4981–4987.
- 8 (a) A. A. Trifonov, E. A. Fedorova, I. A. Borovkov, G. K. Fukin, E. V. Baranov, J. Larionova and N. O. Druzhkov, *Organometallics*, 2007, **26**, 2488–2491; (b) A. A. Trifonov, I. D. Gudilenkov, J. Larionova, C. Luna, G. K. Fukin, A. V. Cherkasov, A. I. Poddol'sky and N. O. Druzhkov, *Organometallics*, 2009, **28**, 6707–6713.
- 9 (a) C. Bianchini, G. Giambastiani, G. Mantovani, A. Meli and D. Mimeo, *J. Organomet. Chem.*, 2004, **689**, 1356–1361; (b) C. Bianchini, D. Gatteschi, G. Giambastiani, I. Guerrero Rios, A. Ienco, F. Laschi, C. Mealli, A. Meli, L. Sorace, A. Toti and F. Vizza, *Organometallics*, 2007, **26**, 726–739; (c) P. Barbaro, C. Bianchini, G. Giambastiani, I. Guerrero Rios, A. Meli, W. Oberhauser, A. M. Segarra, L. Sorace and A. Toti, *Organometallics*, 2007, **26**, 4639–4651; (d) C. Bianchini, G. Giambastiani, I. Guerrero Rios, A. Meli, W. Oberhauser, L. Sorace and A. Toti, *Organometallics*, 2007, **26**, 5066–5078.
- 10 (a) J. Z. Jin, Z. S. Jin, W. Q. Chen and Y. Zhang, *Chinese J. Struct. Chem. (Jiegou Huaxue)*, 1993, **12**, 241–245; (b) A. V. Khvostov, B. M. Bulychev, V. K. Belsky and A. I. Sizov, *J. Organomet. Chem.*, 1999, **584**, 164–170; (c) T. Jiang, Q. Shen, Y. Lin and S. Jin, *J. Organomet. Chem.*, 1993, **450**, 121–124; (d) A. A. Trifonov, E. N. Kirillov, S. Dechert, H. Schumann and M. N. Bochkarev, *Eur. J. Inorg. Chem.*, 2001, 3055–3058.
- 11 (a) S. Wang, Y. Feng, L. Mao, E. Sheng, G. Yang, M. Xie, S. Wang, Y. Wei and Z. Huang, *J. Organomet. Chem.*, 2006, **691**, 1265–1274; (b) J. Cheng, D. Cui, W. Chen, N. Hu, T. Tang and B. Huang, *J. Organomet. Chem.*, 2004, **689**, 2646–2653.
- 12 M. Schultz, J. M. Boncella, D. J. Berg, T. Don Tilley and R. A. Andersen, *Organometallics*, 2002, **21**, 460–472.
- 13 M. Wiebske and D. Mootz, *Acta Crystallogr., Sect. B: Struct. Crystallogr. Cryst. Chem.*, 1982, **38**, 2008–2013.
- 14 (a) R. M. Buchanan and C. G. Pierpont, *J. Am. Chem. Soc.*, 1980, **102**, 4951–4957; (b) A. Dei, D. Gatteschi, C. Sangregorio and L. Sorace, *Acc. Chem. Res.*, 2004, **37**, 827; (c) E. Evangelio and D. Ruiz-Molina, *Eur. J. Inorg. Chem.*, 2005, 2957; (d) O. Sato, J. Tao and Y.-Z. Zhang, *Angew. Chem., Int. Ed.*, 2007, **46**, 2152.
- 15 (a) J. M. Veauthier, E. J. Schelter, C. J. Kuehl, A. E. Clark, B. L. Scott, D. E. Morris, R. L. Martin, J. D. Thompson, J. L. Kiplinger and K. D. John, *Inorg. Chem.*, 2005, **44**, 5911–5920; (b) I. L. Fedushkin, O. V. Maslova, E. V. Baranov and A. S. Shavyrin, *Inorg. Chem.*, 2009, **48**, 2355–2357.
- 16 O. Kahn, in *Molecular Magnetism*, Wiley-VCH, New York, 1993.
- 17 Recent studies conducted on cobalt:dioxolene systems have indeed clearly demonstrated the outstanding importance of both the aggregation state and the local environment around the molecule in determining the temperature at which the valence tautomeric phenomenon occurs. See (a) P. Dapporto, A. Dei, G. Poneti and L. Sorace, *Chem.–Eur. J.*, 2008, **14**, 10915–10917; (b) A. Dei, A. Feis, G. Poneti and L. Sorace, *Inorg. Chim. Acta*, 2008, **361**, 3842–3846; (c) A. Dei, G. Poneti and L. Sorace, *Inorg. Chem.*, 2010, **49**, 3271–3277; (d) Y. Mulyana, G. Poneti, B. Moubaraki, K. S. Murray, B. F. Abrahams, L. Sorace and C. Boskovic, *Dalton Trans.*, 2010, **39**, 4757–4767.
- 18 (a) V. C. Gibson, R. K. O'Reilly, D. F. Wass, A. J. P. White and D. J. Williams, *Dalton Trans.*, 2003, 2824–2830; (b) T. V. Laine, M. Klinga and M. Leskelä, *Eur. J. Inorg. Chem.*, 1999, 959–964; (c) T. V. Laine, U. Piironen, K. Lappalainen, M. Klinga, E. Aitolla and M. Leskelä, *J. Organomet. Chem.*, 2000, **606**, 112–124; (d) C. Bianchini, H. M. Lee, G. Mantovani, A. Meli and W. Oberhauser, *New J. Chem.*, 2002, **26**, 387–397.
- 19 C. J. O'Connor, *Prog. Inorg. Chem.*, 1982, **29**, 103.
- 20 C. Bianchini, G. Giambastiani, L. Luconi and A. Meli, *Coord. Chem. Rev.*, 2010, **254**, 431–455.
- 21 C. Bianchini, G. Mantovani, A. Meli, F. Migliacci and F. Laschi, *Organometallics*, 2003, **22**, 2545–2547.
- 22 (a) Z. Benko, S. Burck, D. Gudat, M. Nieger, L. Nyulaszi and N. Shore, *Dalton Trans.*, 2008, 4937–4945; (b) K. Nienkemper, G. Kehr, S. Kehr, R. Fröhlich and G. Erker, *J. Organomet. Chem.*, 2008, **693**, 3063–3073.
- 23 CrysAlisCCD 1.171.31.2 (release 07-07-2006), CrysAlis171.NET, Oxford Diffraction Ltd.
- 24 A. Altomare, M. C. Burla, M. Camalli, G. L. Cascarano, C. Giacovazzo, A. Guagliardi, A. G. G. Moliterni, G. Polidori and R. Spagna, *J. Appl. Crystallogr.*, 1999, **32**, 115–119.
- 25 G. M. Sheldrick, *SHELXL*, University of Göttingen, 1997.
- 26 M. Nardelli, *Comput. Chem.*, 1983, **7**, 95–98.
- 27 L. J. Farrugia, *J. Appl. Crystallogr.*, 1997, **30**, 565.